Branesh et al. 2021. *Int. J. Vehicle Structures & Systems*, 13(1), 86-90
ISSN: 0975-3060 (Print), 0975-3540 (Online)
doi: 10.4273/ijvss.13.1.17

International Journal of Vehicle Structures & Systems
Available online at www.maftree.org/eja

Numerical Study of Scramjet Combustor with Tandem Dual Cavity for Non-Reactive Jets

Ajin Branesh[a], Jeevanjot Kaur[b] and Akashdeep Singh

Dept. of Aerospace Engg., Chandigarh University, Mohali, Punjab, India
[a]Corresponding Author, Email: ajin.e8705@cumail.in
[b]Email: jeevanjotkaur016@gmail.com

ABSTRACT:

In the past decades, flame out is a major phenomenon that paves way for high fuel consumption in scramjet combustion. For enhancing mixing and flame holding characteristics, different types of cavities are introduced in a scramjet combustion chamber which can hold air for a bit and acts like an atomizer. For increasing the combustion efficiency and burnout ratios, recirculation is maintained by using cavity and ramp angle techniques. In this paper, numerical analysis has been carried out for two dimensional non-reacting flows in the combustor of scramjet engine with tandem dual cavity that creates high turbulent kinetic energy for ensuring combustion stability. This work is an enlightened approach for predicting the flow phenomenon that induces re-circulations after implementing various tandem dual cavities with varying length to diameter ratio and ramp angle. These in turn overcome the low mixing rates due to compressibility effects at high convective Mach number.

KEYWORDS:

Non-reactive flows; Tandem dual cavity; Burnout; Ramp angle; Scramjet combustor

CITATION:

A.A. Branesh, J. Kaur and A. Singh. 2021. Numerical Study of Scramjet Combustor with Tandem Dual Cavity for Non-Reactive Jets, *Int. J. Vehicle Structures & Systems*, 13(1), 86-90. doi:10.4273/ijvss.13.1.17.

1. Introduction

At hypersonic speeds, when the air enters the inlet at a speed higher than speed of sound, combustion takes place at supersonic conditions. So the time remains for the flame to achieve stability in the combustion chamber is of on an average 8-10 milliseconds. Some injection techniques are used to have better mixing such as vanes, backward facing steps, swirl, and tube mixers. Many researches were conducted to increase the combustion stability with reduced time interval and increasing the efficiency of air fuel mixture. Some of the previous studies suggest that the length of the cavity is proportional to the mass entertainment rate and the depth corresponds to the residence time [1]. Further reviews are given in [3-6] which relates the reactive and non-reactive flow field for open and closed cavities along with their behaviour with ignition of fuels. This suggests various L/D ratios for predicting the crucial time to initiate the ignition [2]. The purpose of this paper is to predict the exact shape configuration that induces combustion instability from the non-reactive flow flied behaviour and can be suggested for reactive flow field simulations that paves results of exact combustion mixer in the above mentioned model configuration.

For predicting the non-reactive flow field containing strong pressure gradient, RANS method, SST k-ω turbulence model is used for all cases [5]. The base framework is gathered from the scramjet test model developed by China Aerodynamics and Research and Development Centre (CARDC). The test model was composed by an isolator and a combustor as shown in Fig. 1. The length and height of the isolator are 200mm and 18mm respectively. The combustor was composed of a constant straight section with 80mm long and 24mm high and a diffusion section with 220mm long. 7 fuel-jet holes were placed in the bottom wall of the combustor equidistantly, with a diameter of 1.2mm and the beginning location is 65mm from the combustor inlet [7]. The configuration of combustor is shown in Fig. 2.

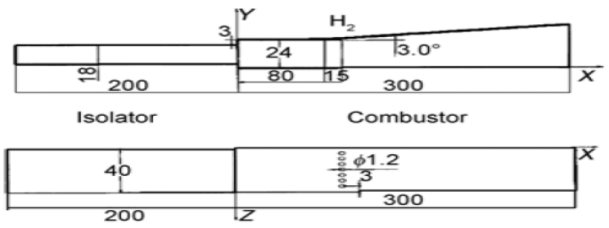

Fig. 1: Combustor rig configuration

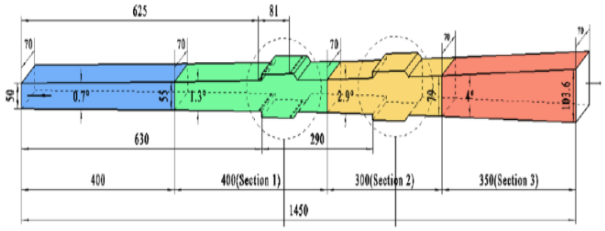

Fig. 2: 3D configuration of combustor

For simulation, all the cases with full size are considered and for better accuracy and time consideration, fine structured grids are used at the

positions were shock interactions occurs and near to the cavities as well. The remaining combustor is modeled with coarse structured grids all around as shown in Fig. 3. The number of elements and nodes contained in each model is 139890 and 141394. Assuming the incoming flow velocity as constant and the boundary conditions are set as pressure inlet and pressure outlet [8-9]. At the walls, adiabatic and no slip boundary conditions are enabled [10]. The simulations for all cases are carried out without fuel jet combustion. Due to the implementation of cavity, series of expansion waves are produced and are interacted near the mid plane axis of the combustor. More over the intensity of shockwaves are getting reduced further as it travels throughout the length of the combustor [11]. The comparative data, as given in Table 1, are available to ensure the better cavity configuration for enhanced flame holding characteristics.

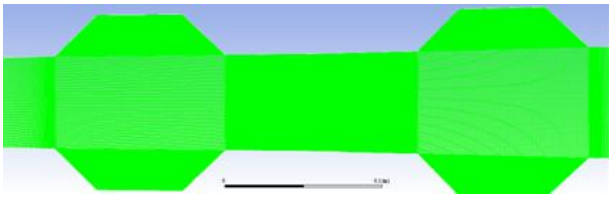

Fig. 3: Computational grid domain

Table 1: Cavity dimensions and specifications

Case	L/D	Incident angle	Ramp angle
1	5	90	45
2	8	90	45
3	7	90	55
4	3.6	90	15
5	3	45	45
6	7	90	30
7	4.4	16	45

2. Results and discussion

As shown in Fig. 4, pressure is nearly constant on the leading edge cavity but has increased due to shock wave at the trailing edge of cavity an increment of pressure. A gradual increase in area leads to drop in pressure up to second cavity. In second cavity, the pressure has decreased but due to shockwave, a sudden increase in the pressure is observed. Then after, the pressure decreases as shown in Figs. 5 and 6. Results show a small pressure drop after cavity which can be due to formation of weak shock wave. With L/D = 7 and ramp angle of 30°, there is a formation of weak shock which leads to reduction in the pressure. Pressure in the cavity varies very much as shown in Fig. 7. Pressure in first cavity has lower value but due to shockwave formation at the trailing edge, the pressure increases. The same pattern is observed in the second cavity. In the second cavity, the pressure drop takes place at some regions as shown in Figs. 8 and 9.

The velocity contour of first and second cavity is different. In the first cavity at upper surface near the leading edge, the velocity is high but at the trailing edge it drops. There are small losses in the velocity along the cavities due to formation of shockwave as shown in Fig. 10. Fig. 11 shows the velocity is nearly same as in the first cavity. But in the second cavity fluctuation are observed due to recirculation [12].

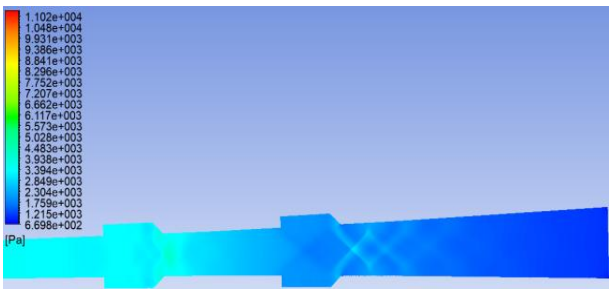

Fig. 4: Pressure contour for dual cavity case 1

Fig. 5: Pressure contour for dual cavity case 2

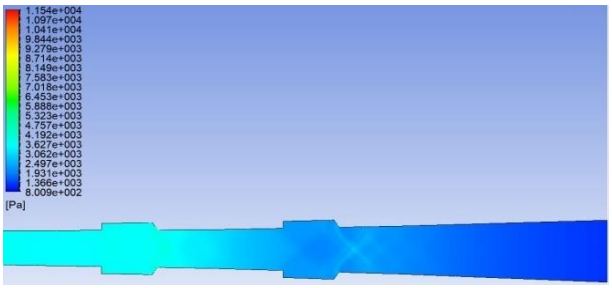

Fig. 6: Pressure contour for dual cavity case 3

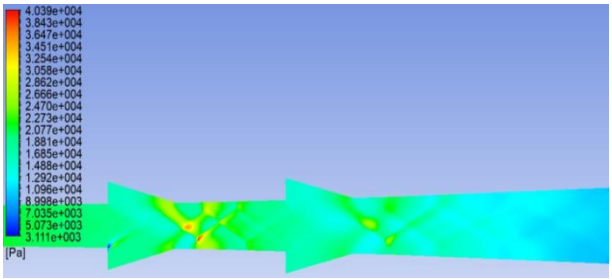

Fig. 7: Pressure contour for dual cavity case 4

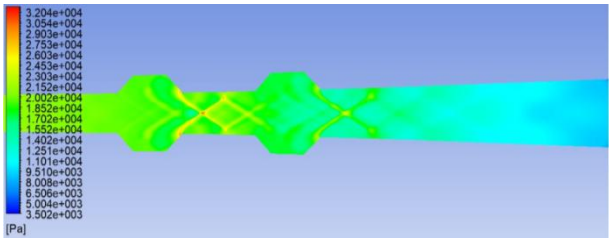

Fig. 8: Pressure contour for dual cavity case 5

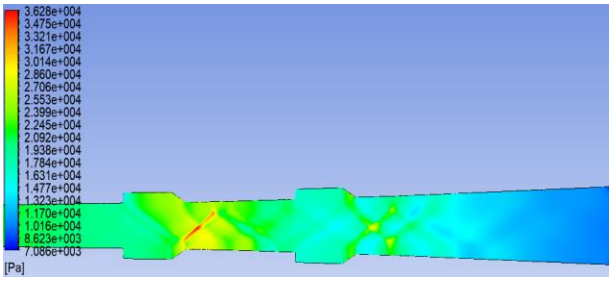

Fig. 9: Pressure contour for dual cavity case 6

Velocity is nearly same as in the first cavity and varies in the second cavity due to formation of shockwave as shown in Fig. 12. Fig. 13 shows that the velocity is very less in the cavity with trace of recirculation, which increases the mixing time. The penetrating velocity does have an impact on dual cavity implementation for this case and results predict an effective one for practical use in Figs. 14 to 16.

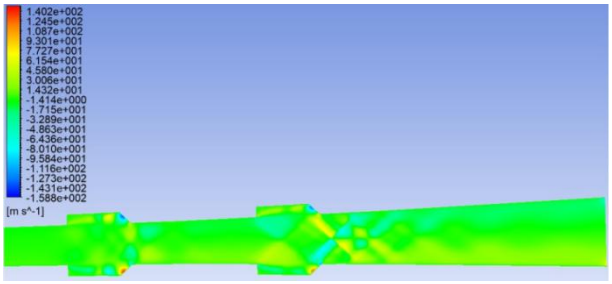

Fig. 10: Velocity contour for dual cavity case 1

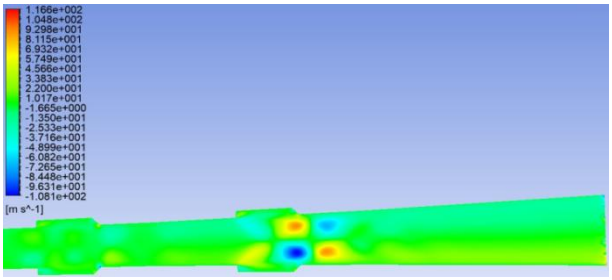

Fig. 11: Velocity contour for dual cavity case 2

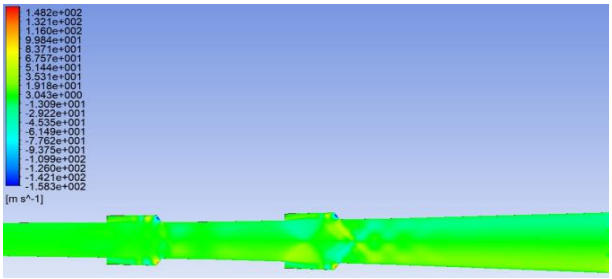

Fig. 12: Velocity contour for dual cavity case 3

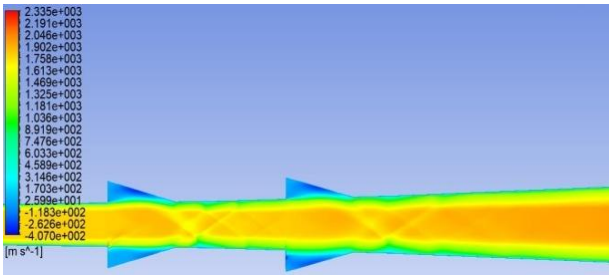

Fig. 13: Velocity contour for dual cavity case 4

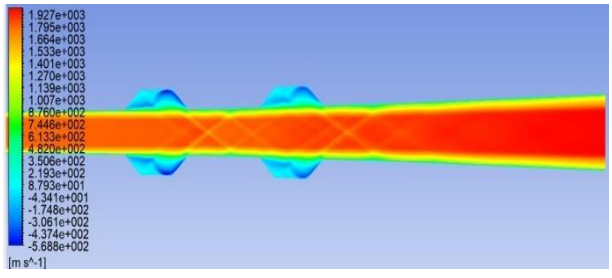

Fig. 14: Velocity contour for dual cavity case 4

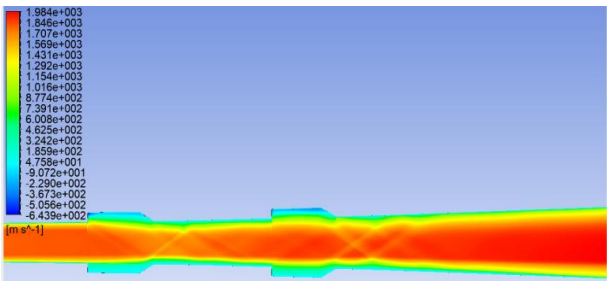

Fig. 15: Velocity contour for dual cavity case 5

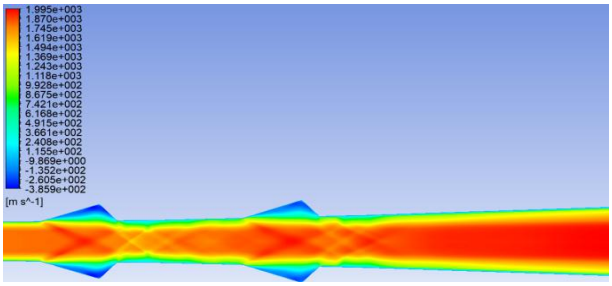

Fig. 16: Velocity contour for dual cavity case 6

As seen in Fig. 17, the first case continuously represents an impact of turbulence with an increase in value near the trailing edge which increases mixing near trailing edge. Turbulence kinetic energy in first cavity near the wall is same as in first case but in second cavity it changes near trailing edge and poses high rate as observed in Fig. 18.

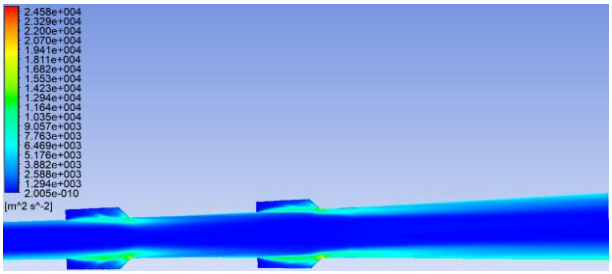

Fig. 17: Turbulence kinetic energy for case 1

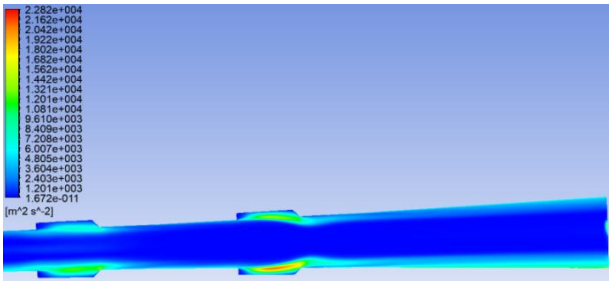

Fig. 18: Turbulence kinetic energy for case 2

Fig. 19 shows that the turbulence kinetic energy is nearly constant in cavities and has small changes near trailing edge. Turbulent energy remains nearly constant along the axis. On the slanting section of the cavity, turbulence is more which results in slightly longer mixing time [13]. Comparing the existing model, this can in Fig. 20 can be a recommended option. This phenomenon clearly displays symmetry of reactions and flow pattern coinciding exactly with the axis of flow which may be an essential tool for increasing the mixing time as observed in Fig. 21. In Fig. 22 to Fig. 24, the recirculation zone experiences better turbulence which

delays the mixing time and provides better atomizing capabilities. The impact intensity is more as the flow experiences sudden turbulent because of the slanting section employed on the frontal face.

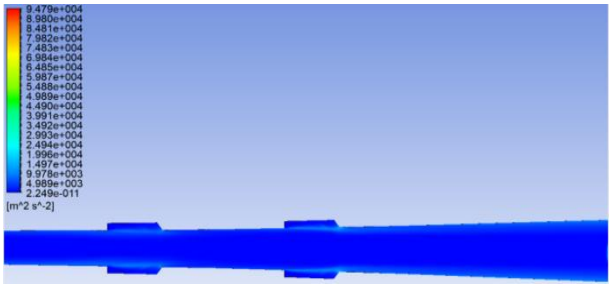

Fig. 19: Turbulence kinetic energy for case 3

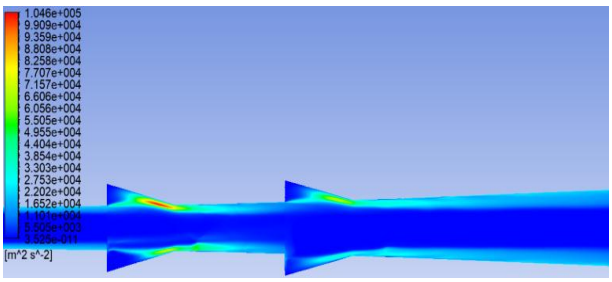

Fig. 20: Turbulence kinetic energy for case 4

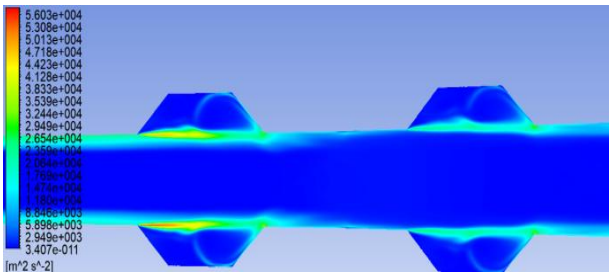

Fig. 21: Turbulence kinetic energy for case 4

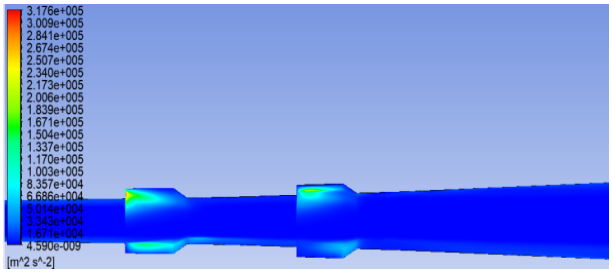

Fig. 22: Turbulence kinetic energy for case 5

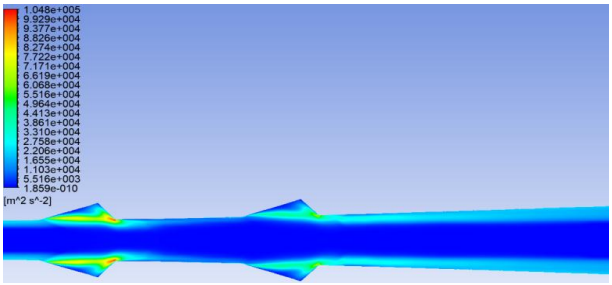

Fig. 23: Turbulence kinetic energy for case 6

Density in first cavity is high and in second cavity density is low. Moreover along the axis, the density starts to decrease in a divergent manner as shown in Fig. 24. Fig. 25 shows a better visualization of constant density pattern throughout the domain which has a desired aspect of flow. An identical density stream is focused similar to case 1 and has enough evidence for enhanced shocks as shown in Fig. 26. Fig. 27 shows that the case slightly slowed down in the density intensity as the flow is impelled throughout the second cavity. Maximum values are experienced in Fig. 28, as the flow is imparted after the first cavity which is also repelled back in the next cavity with a more prominent increase in density.

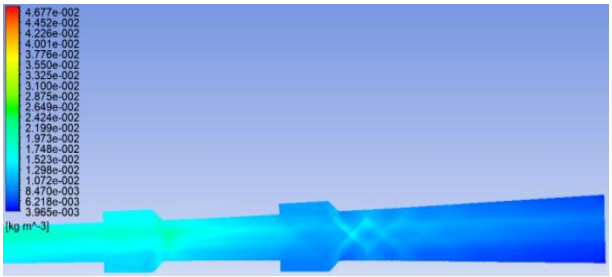

Fig. 24: Density contour for case 1

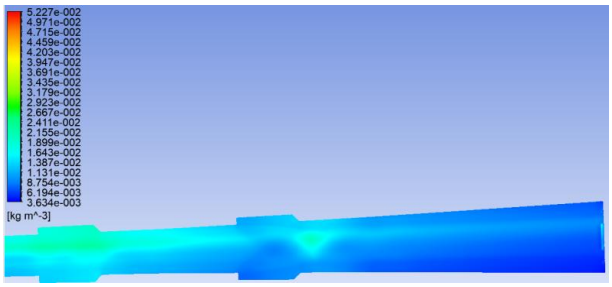

Fig. 25: Density contour for case 2

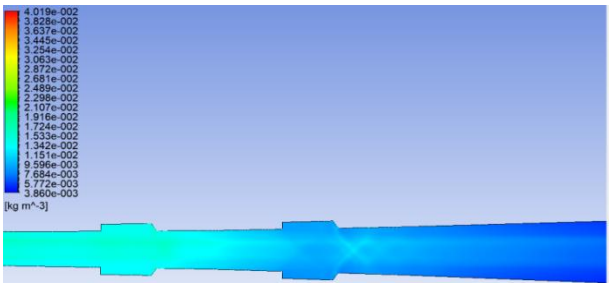

Fig. 26: Density contour for case 3

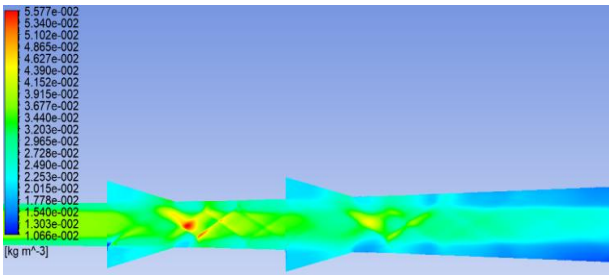

Fig. 27: Density contour for case 4

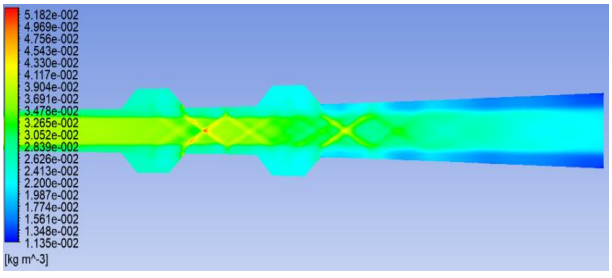

Fig. 28: Density contour for case 5

Slight increases to a value of 2.322×10^{-2} kgm^{-3} can be observed after the first due to shockwave formation and remains nearly constant in the second cavity as shown in Fig. 29. This configuration is exactly the opposite of case 4 which experiences a continuous enhancement of density after the first section and repelled simultaneously towards the exit of the model as observed in Fig. 30.

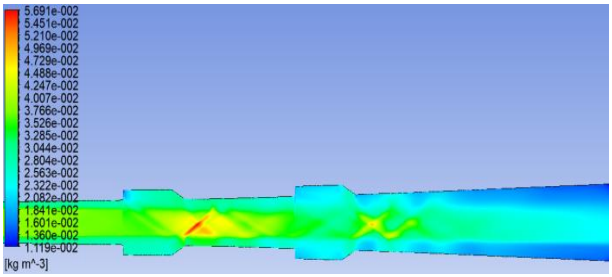

Fig. 29: Density contour for case 6

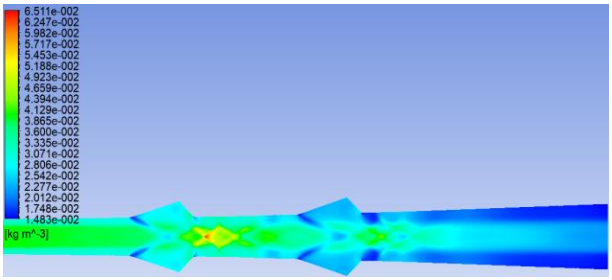

Fig. 30: Density contour for case 7

3. Conclusion

Analysis has been carried out with models of cavities with different configuration of L/D and ramp angle. It is noted that last three models experiences better velocity ratio without major losses in exit jet velocities. Based on density effects, the last four models can be taken into consideration for further analysis as it gives predominant values. The turbulence kinetic energy is better for the last three models which ensure the delayed time based on turbulence criterion. This leads to more recirculation and vortex formation directly results in more mixing. The changing behavioural pattern of flow inside the domain with various configurations depicted well the flow behaviour of non-reactive jets.

REFERENCES:

[1] J.Y. Choi, F. Ma and V. Yong. 2005. Combustion oscillations in a scramjet engine combustor with transverse fuel injection, *Proc. Combustion Institute*, 30, 2851-2858. https://doi.org/10.1016/j.proci.2004.08.250.

[2] W. Lu, Q. Zhansen and G. Liangjie. 2015. Numerical study of the combustion field in dual-cavity scramjet combustor, *Procedia Engg.*, 99, 313-319. https://doi.org/10.1016/j.proeng.2014.12.540.

[3] D. Kumar and Dr. K. Choudhary. 2017. Numerical simulation of scram-jet combustor using double wall injector, *Int. J. Res. in Applied Sci. & Engg. Tech.*, 5(5), 1566-1570.

[4] A. Ben-Yakar and R.K. Hanson. 2001. Cavity flame holders for ignition and flame stabilization in scramjets: An overview, *AIAA J. Propulsion and Power*, 17(4), 869-877. https://doi.org/10.2514/2.5818.

[5] S.K. Dixit, R.K. Choudhary and S. Badholiya. 2017. Mathematical modeling and analysis of different type of fuel injector in scramjet engine using CFD simulation in Fuent, *Int. J. Applied Sci., Engg. & Tech*., 5(2), 379-389.

[6] X. Zhang and J.A. Edwards. 1992. Experimental investigation of supersonic flow over two cavities in tandem, *AIAA J.*, 30(5), 1182-1190. https://doi.org/10.2514/3.11049.

[7] H.I.H. Saravanamuttoo, G.F.C. Rogers, P. Straznicky, H. Cohen and A.C. Nix. 2017. *Gas Turbine Theory*, 5th Ed.

[8] F.S. Billig. 1993. Research on supersonic combustion, *J. Propulsion and Power*, 9(4), 499-514. https://doi.org/10.2514/3.23652.

[9] J.M. Tishkoff, J.P. Drummond, T. Edwards and A.S. Nejad. 1997. Future direction of supersonic combustion research: Airforce on supersonic combustion, *Proc. AIAA 35th Aerospace Sci. Meeting and Exhibit*, Reno, Nevada, USA. https://doi.org/10.2514/6.1997-1017.

[10] R.P. Fuller, P. Wu, A.S. Nejad and J.A. Schetz. 1998. Comparison of physical and aerodynamic ramps as fuel injectors in supersonic flow, *J. Propulsion and Power*, 14(2), 135-145. https://doi.org/10.2514/2.5278.

[11] A. Ben-Yakar. 2000. *Experimental Investigation of Transverse Jets in Supersonic Cross*, Ph.D. Dissertation, Dept. of Mech. Engg., Stanford University, CA.

[12] J.C. McDaniel and J. Graves. 1988. Laser-induced-fluorescence visualization of transverse gaseous injection in a non-reacting supersonic combustor, *J. Propulsion and Power*, 4(6), 591-597. https://doi.org/10.2514/3.23105.

[13] T.E. Parker, M.G. Allen, R.R. Foutter, D.M. Sonnenfroh and W.T. Rawlins. 1995. Measurements of OH and H_2O for reacting flow in a supersonic combusting ramjet combustor, *J. Propulsion and Power*, 11(6), 1154-1161. https://doi.org/10.2514/3.23954.